Ionic liquids enhance electrical conductivity of greases: an impedance spectroscopy study

Akepati Bhaskar Reddy [a,*], Faiz Ullah Shah [b], Johan Leckner [c,a], Mark W. Rutland [d,e,f], Sergei Glavatskih [a,f,g]

[a] *KTH Royal Institute of Technology, Department of Engineering Design, Stockholm 100 44, Sweden*
[b] *Luleå University of Technology, Chemistry of Interfaces, Luleå 97 187, Sweden*
[c] *Axel Christiernsson International AB, Nol 449 11, Sweden*
[d] *KTH Royal Institute of Technology, Division of Surface Chemistry and Corrosion Science, Department of Chemistry, Stockholm 100 44, Sweden*
[e] *Ecole Centrale de Lyon, Laboratoire de Tribologie et de Dynamique des Systèmes, Ecully 69134, France*
[f] *University of New South Wales, School of Chemistry, Sydney 2052, NSW, Australia*
[g] *Ghent University, Department of Electromechanical, Systems and Metal Engineering, Ghent 9052, Belgium*

HIGHLIGHTS

- Ionic liquids enhance the electrical conductivity of lubricating greases.
- The grease conductivity depends upon ion dissociation as well as the ion-grease matrix interactions.
- Lubricating grease electrical conductivity measured through Electrochemical Impedance Spectroscopy.
- The approach allows for the tuning of the electrical properties of greases over many orders of magnitude.

GRAPHICAL ABSTRACT
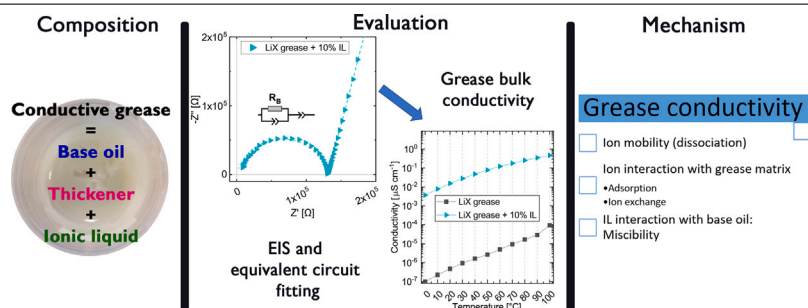
ARTICLE INFO

ABSTRACT

Ionic liquids (ILs) have emerged as viable solutions for developing new-age lubricants, both as neat lubricants and lubricant additives. Enabled by the presence of discrete ions, ILs have the possibility to render electrically conductive lubricants, which is a feasible strategy for developing lubricant systems compatible with modern e-drive conditions. However, this requires the characterization of the electrical properties of lubricants, which is a bottleneck for developing electrically conductive greases, given their complex architecture. This work introduces an electrochemical impedance spectroscopy measurement methodology to evaluate grease samples' electrical properties. Compared to the commonly used conductivity meters, this method, through its multi-frequency alternating current (AC) impedance approach, can effectively distinguish the individual contributions of the bulk and the sample-electrode interface to the measured electrical response. Impedance spectra of grease samples are obtained using an electrochemical cell with parallel plate electrodes, mounted on a temperature-controlled cell stand and coupled with a potentiostat. The grease's bulk conductivity is extracted by fitting the impedance data to relevant equivalent electrical circuits. The bulk conductivity of lithium complex grease doped with ILs is evaluated and compared to greases with conventional conductivity additives (copper powder and conductive carbon black). The analysis of temperature-dependent conductivity reveals the rather different conductivity mechanisms for different additives. For greases doped with ILs, a comparison against the electrical conductivity of neat ILs reveals that, in addition to the ion dissociation, the interaction of the ions with the different grease components (base oil, thickener) is crucial in defining the grease conductivity.

* Correspondence to: KTH Royal Institute of Technology, Department of Engineering Design, Brinellvägen 85, 100 44 Stockholm, Sweden.
E-mail address: abreddy@kth.se (A.B. Reddy).

1. Introduction

Ionic liquids (ILs), generally defined as organic salts existing as liquid below 100 °C [1], have gained popularity in various industrial applications [2]. Being composed of discrete ions, ILs exhibit tunable properties through smart combinations of both cations and anions [3, 4]. The IL properties, such as nonvolatility, nonflammability, and low melting point, have made them a promising choice for developing novel lubricants. Some ILs have been reported to improve lubrication, both as neat lubricants and as additives [4–7]. Furthermore, composed of dissociated ions, ILs are expected to provide electrically conductive pathways through the lubricant film [8]. In recent years, this possibility has become more relevant with the advancements in electric mobility (e-mobility), where extensive research has been reported on bearing damages caused by electric current passage, circulating currents, and electrostatic discharges [9–13]. Approximately 40% of motor failures in electric vehicles (EVs) and hybrid electric vehicles (HEVs) have been reported to be caused by premature bearing failure, primarily due to complex shaft voltages and bearing currents [11]. A high-energy electrical discharge occurs when the voltage buildup exceeds the breakdown potential of an insulating lubricating film in an electrified tribological contact, which could cause catastrophic surface damage [14,15]. Some lubricants have been shown to undergo chemical changes and decomposition in the presence of electric fields, leading to corrosion of steel bearing surfaces [16]. Using electrically conductive lubricants is one of the measures identified to mitigate, if not eliminate, these problems [11]. Other measures could be insulation of the tribo surfaces and grounding of the machine components [11].

Conductive lubricants are expected to prevent voltage build-up across the lubricating film, thereby preventing electrical discharge breakdowns [17,18]. Nevertheless, high lubricant conductivity might not always be the best option. Contacts with a low resistivity lubricant ($< 10^5$ Ω m, i.e., conductivity > 1 μS cm^{-1}) have been reported to experience tribo-corrosion, gradually leading to "fluting" damage, when exposed to specific conditions of periodic currents [19]. It is therefore recommended that an EV lubricant must be moderately conductive to remove static charge, but not highly conductive which can cause current leakage and short-circuiting [20]. Gao et al. have suggested two different lubricant formulations to be used in EVs and HEVs: (1) a high conductivity lubricant (3×10^{-5} to 2×10^{-4} μS cm^{-1} at room temperature) for minimizing electrical charge buildup and protecting against spark-related wear in high voltage components [21]; and (2) a low conductivity lubricant (5×10^{-7} to 3×10^{-5} μS cm^{-1} at room temperature) for minimizing electrical charge leakage and drain down of energy storage devices [22]. Therefore, a generalized conductive lubricant solution would not be feasible due to the diverse tribological conditions and electrical conditions. Instead, the development of designer conductive lubricants could ensure the longevity and reliability of machine components exposed to electrical currents and voltages. To create these designer solutions, the electrical properties of the lubricant must be evaluated and tuned to meet the specific application requirements.

Greases, which are semi-solid lubricants formed as a dispersion of thickening agents (thickeners) in a liquid lubricant (base oil), have been common lubricants used in vehicles. Therefore, they are key lubricants in electrical drivetrains as well [23]. A grease thickener generally forms a three-dimensional microstructure that traps the base oil and provides the grease with the appropriate rheological and tribological characteristics [24]. According to the NLGI grease production survey report for 2022 [25], lithium soaps are the most widely used grease thickener in production, accounting for approximately 62% of grease production volume. Due to this complex architecture, greases with specific properties (like electrically conductive) are difficult to design and investigate. There have been several approaches to the development of conductive lubricating greases using conductive materials, such as graphite or nano-carbon [18,26–28], carbon nanotubes

(CNT) [29–33], metal and metal oxides (copper, silver, antimony-doped tin oxide) [34], either as a thickener matrix or additives. Although these options provide conductive pathways, some of them result in deterioration of lubrication and wear-resistant properties. Beyond certain additive concentrations, carbon-based greases (with carbon black and CNTs) exhibit increased friction and wear [26,31,32]. Additionally, to form electrically conductivity greases with CNTs, a high CNT concentration would be required so that they could form 3-D networks through Van der Waals interactions [30]. When conductive particles are added to grease, mechanical wear increases, making the lubricant less effective and often leading to premature failure [34,35]. These limitations, which restrict the implementation of conductive greases for addressing electrically induced surface damages, can be eliminated by using ILs. ILs have been implemented in the development of electrically conductive greases, either as base oil [28,36,37], or as additives to conventional greases [38–41]. Greases containing IL additives have been demonstrated to possess improved tribological characteristics, such as decreased friction and wear [38,39,41–46].

Although several well-defined methods have been established for evaluating the electrical properties of liquid samples (standards like ASTM D4308 Standard test method for electrical conductivity of liquid hydrocarbons by precision meter [47]; ISO 15091:2019 Paints and varnishes — Determination of electrical conductivity and resistance [48]; ASTM D2624 Standard test method for electrical conductivity of aviation and distillate fuels [49]), there is no standardized method to quantify the electrical conductivity of greases. Most of the studies reported for conductive greases measure conductivity using conventional conductivity meters [26,28,30–32,34,36–41,50]. Although being fast, inexpensive, and non-destructive, these methods require either instantaneous measurement or alternating current (AC) measurement to minimize errors due to ion depletion and polarization. They are also limited in terms of accuracy at low electrical conductivity levels. These methods are, therefore, not suitable for samples that exhibit complex impedance (frequency-dependent) and/or contributions from interfacial structuring processes (like diffusion) at the electrode-sample interface. Electrochemical impedance spectroscopy (EIS), which is a multi-frequency AC electrochemical measurement technique, is an efficient method to evaluate the electrical characteristics of material-electrode systems [51]. The multifrequency approach permits the separation of the electrical contributions from the bulk matrix and the interfacial structuring (and dynamic processes) to the system's conductivity. The bulk properties and electrode effects are generally associated with the frequency range's high- and low-end, respectively. The impedance data can be fitted to equivalent electrical circuits, which act as fingerprints of the sample and help extract valuable information about the bulk material's electrical properties and the electrode-sample interface [52,53]. EIS has been successfully applied to a wide range of complex systems, such as cement and concrete [54–59], ceramics and composites [60], and polymeric electrolytes [61]. It has also been used to measure the conductivity and capacitance of lubricating oils with additives [62].

In this research, we thus use EIS to assess the electrical characteristics of greases since this allows the relevant information to be obtained without a detailed molecular picture of the grease structure, and importantly, separating the interfacial effects from the bulk. ILs have been presented as a means for enhancing the conductivity of greases, comparing them with conventional nonionic conductivity additives (copper powder and conductive carbon black). The greases used in this investigation are built on a lithium complex thickener, a widely used type of grease thickener [25]. The study employs temperature-dependent EIS-based electrical conductivity measurements, which provide valuable insights into the underlying conductivity mechanisms and pathways. This understanding plays a crucial role in selecting the most suitable materials for designing application-specific electrically conductive greases.

Table 1
Base grease properties.

Property		LiX-10
Thickener type		Lithium complex
Thickener content [%]		20.6%
Base oil composition [wt%]		93.7 PAO-10 + 6.3 Adipate ester
Base oil Viscosity [mm^2 s^{-1}]	@ 40 °C	61.4
	@ 100 °C	9.4
	NLGI grade	2

2. Methods and materials

2.1. Greases

A model lithium complex grease with a non-polar base oil (PAO-10) was produced using a method described elsewhere [63,64]. The choice of thickener was made in light of the fact that lithium soaps are by far the most common type on the market [25]. The lithium complex thickener is made up of a lithium 12-hydroxystearate complexed with a dilithium azelate. A small amount of adipate ester (6.3%) was added to the base oil to ensure a rapid and complete saponification reaction through increased base oil polarity. Table 1 gives an overview of the properties of the grease. The grease was produced in a pilot reactor as described elsewhere [63].

Five ILs were selected for this study. Four of these ILs were based on a phosphonium cation decorated with long alkyl chains, while the remaining one was based on an imidazolium cation. The molecular structures, designations and respective sources of ILs are given in Table 2. We selected P-BOB, P-BMB, and P-DCA based on their promising tribological properties when used as grease additives, as reported by Ploss et al. [43]. P-BEHP was selected because of its popularity in tribological research [46,67], and its shown ability to enhance the electrical conductivity of automatic transmission fluids [8]. In addition to these, EMIM-TFSI was studied as a comparator because its reported conductivity [68] is multiple orders of magnitude higher than that of the orthoborate ILs P-BOB and P-BMB [65,66]. This choice of ILs provides a wide range of additive conductivity to evaluate the proposed methodology. Visual checks were conducted on 10 wt% solutions of these ILs and the base oil (93.7 PAO-10 + 6.3 Adipate ester) to assess their miscibility. The results revealed that only P-BEHP showed miscibility with the base oil at this concentration.

To compare the results with traditional non-ionic additives, two grease samples with copper powder (Rogal Copper GK 0/50, Schlenk Metallic Pigments GmbH) and conductive carbon black (ENSACO 250G, Imerys Graphite & Carbon Switzerland Ltd.) as additives were also tested.

Ploss et al. demonstrated that the tribological benefits from ILs were much more pronounced when the IL concentration was high (10 wt%) [43]. Therefore, the ILs and solid additives were blended into the grease, at 10% wt concentration, using a DAC600 SpeedMixer. The mixing was carried out in three steps, where grease was manually mixed using a spatula between steps. This was done to ensure that heavy components, like the copper powder, would blend properly into the grease matrix.

2.2. Impedance spectroscopy

To obtain the impedance spectra of grease samples, a TSC battery cell (RHD instruments, Germany) in a two-electrode configuration (Fig. 1) was used with a Metrohm Autolab (PGSTAT302N) electrochemical workstation equipped with FRA32M module for impedance spectroscopy. The grease sample was sandwiched between two stainless steel disk electrodes with a contact area of 8 mm in diameter within the battery cell. The size of the sample was controlled by using an 80 μm thick PEEK (Polyether ether ketone) spacer that had an internal
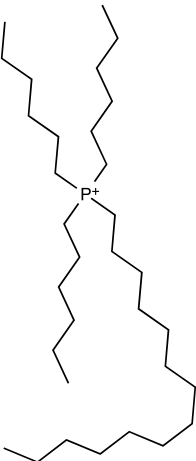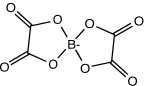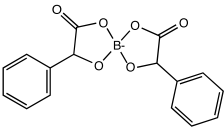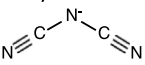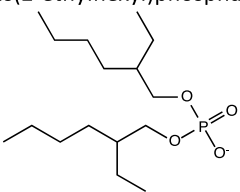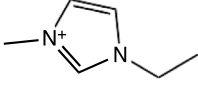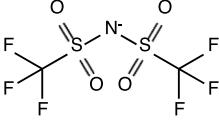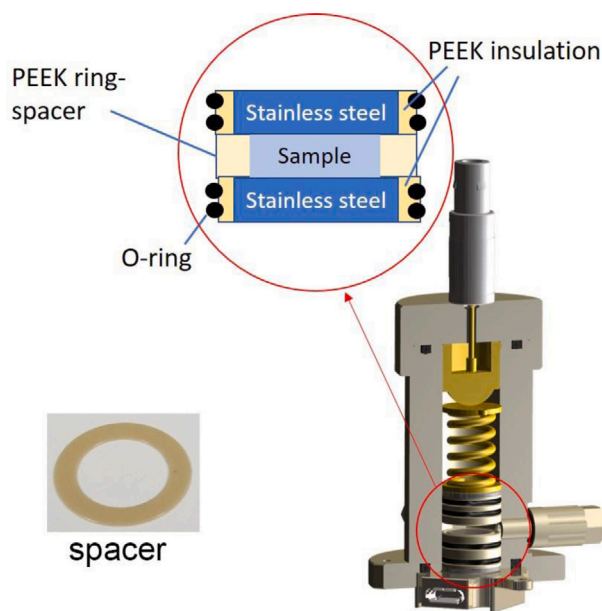

Fig. 1. Schematics of TSC battery cell. The cell is in a two-electrode configuration with the sample sandwiched between two parallel stainless steel electrode plates, with a constant separation maintained through a PEEK spacer and packed with a screw cap and spring mechanism.

diameter of 8 mm and an external diameter of 12 mm. The cell was packed with a screw cap and the contact pressure was adjusted with a gold-plated spring (2.3 N mm^{-1} spring constant). The screw cap was tightened by two turns, resulting in a force of 4.6 N acting on an area of 1.13 cm^2. The total contact pressure applied to the sample was about 40 kPa. The cell constant for the battery cell, i.e., the ratio of spacer thickness and the exposed area of the electrode, was calculated to be 0.016 cm^{-1}. Impedance measurements for grease samples were performed in the frequency range of 0.1 Hz to 1 MHz with an AC amplitude of 10 mV$_{rms}$.

The cell was mounted on a Microcell HC cell stand (RHD instruments, Germany) coupled with a Peltier element-enabled temperature controller unit. Experiments were performed in the temperature range of 0 to 100 °C. Before each experiment, the electrodes were polished with a Kemet diamond paste (0.25 μm). Impedance responses of four temperature sweeps, alternating between heating and cooling (hereinafter referred to as 1-Heating, 2-Cooling, 3-Heating, and 4-Cooling sweeps), were recorded. The cells were thermally equilibrated for at least 10 min before each measurement. The measured impedance data were recorded using the NOVA 2.1 software.

The obtained impedance spectra were visualized and analyzed using RelaxIS3 software from RHD Instruments. The characteristics of the Nyquist impedance plots (the real part of impedance plotted against the imaginary part at a series of frequencies) were evaluated to establish relevant equivalent circuits that would reflect the bulk and the interfacial electrical properties. The equivalent circuits were composed of electrical circuit elements like resistors, constant phase elements (CPEs), and Warburg elements. CPEs are general circuit elements with a constant phase angle (0° for a resistor, −90° for a capacitor, or +90° for an inductor) [69]. Here, CPEs are used to represent imperfect bulk capacitance and double-layer capacitance at the electrode interface. The non-ideal behavior can be attributed to various factors such as surface roughness, non-uniform current and potential distribution, electrode porosity, and deviations due to the oxide layer [70]. The impedance of a CPE can be expressed as: $Z_{CPE} = \frac{1}{(i\omega)^\alpha Q}$; where Q is the admittance value and α is an exponent generally between 0.9 and 1 ($\alpha = 1$ for ideal

Table 2
Molecular structures of the ILs.

Cation	Anion	Designation	Source
trihexyl(tetradecyl)phosphonium	bis(oxalato)borate	**P-BOB**	[65]
	bis(mandelato)borate	**P-BMB**	[66]
	dicyanamide	**P-DCA**	*Cytec*
	bis(2-ethylhexyl)phosphate	**P-BEHP**	*Iolitec*
1-Ethyl-3-methylimidazolium	bis(trifluoromethylsulfonyl)imide	**EMIM-TFSI**	*Iolitec*

capacitor). A Warburg element is commonly used to describe semi-infinite linear diffusion, i.e., unrestricted diffusion to a large planar electrode [71]. The impedance of a Warburg element can be expressed as: $Z_W = \frac{A_W}{\sqrt{\omega}} - i\frac{A_W}{\sqrt{\omega}}$; where A_W is the Warburg-coefficient. The impedance of the resistor is equal to its resistance and is independent of the AC frequency (ω). The elements could be combined in various configurations, a combination of series and parallel arrangements, to correspond to the various features of the measured impedance spectra. For example, an offset from zero could be represented by a resistor, an inclined straight line could be described by a double-layer capacitance (CPE) or diffusion (Warburg element), while a semi-circular feature could be represented by an RC circuit (resistor and capacitor in parallel), or by an RP circuit (resistor and CPE in parallel) in case of a "depressed" semicircle.

The impedance data were fitted to the equivalent electrical circuits to obtain values for the different circuit elements. The bulk conductivity was extracted from the fitted value for the resistor of the part of the circuit representing the bulk properties. The conductivity, σ μS cm^{-1}, was calculated as: $\sigma = \frac{k}{R} \times 10^6$; where k is the cell constant in cm^{-1} and R is the fitted resistance in Ω.

For the evaluation of the ionic conductivity of neat ILs, a TSC 70 cell (RHD instruments, Germany) was used. This cell was also setup in a two-electrode configuration, with a 0.25 mm platinum wire as the working electrode and a 70 μL platinum cup as a sample container and as a counter electrode (Fig. 2). Impedance measurements were performed in the frequency range from 1 Hz to 1 MHz with a 10 mV$_{rms}$ AC voltage amplitude. The cell constant of the liquid cell, $K_{Lcell} = 18.54$ cm^{-1}, was determined by using a 100 μS cm^{-1} KCl standard solution from Metrohm.
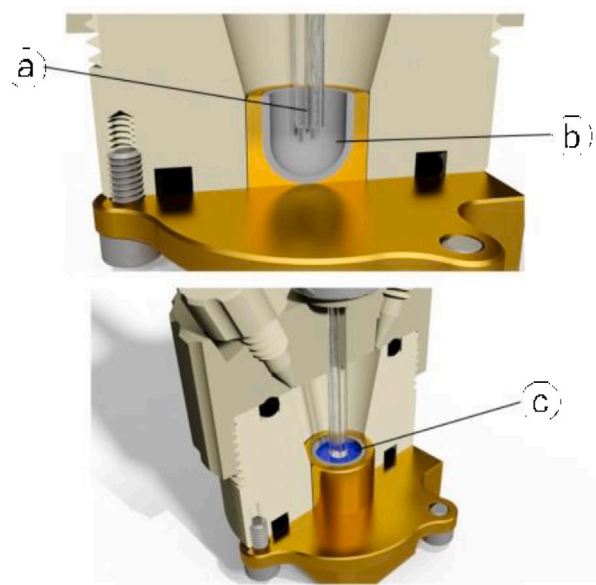

Fig. 2. Schematics of TSC 70 cell. The cell uses a two-electrode configuration with a 0.25 mm platinum wire working electrode (a); 70 μL platinum cup (b) acting as a counter electrode while also holding the liquid sample (c).
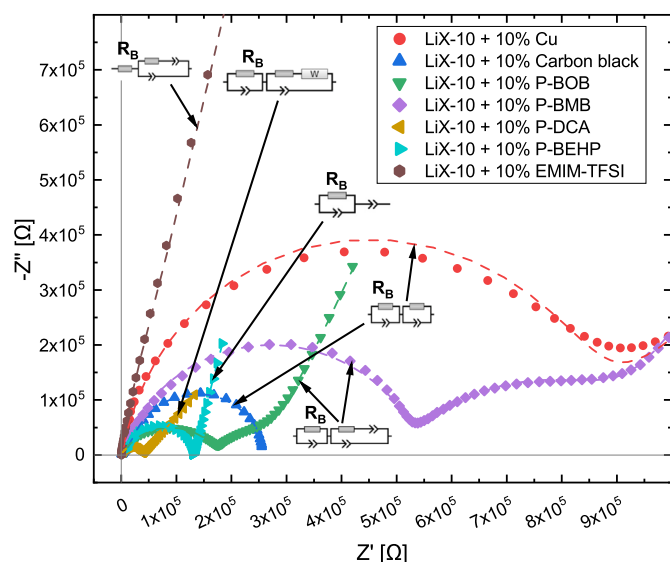
Fig. 3. Impedance spectra Nyquist plots for the grease samples at 60 °C during 3-Heating temperature sweep, and the respective equivalent electrical circuits.

3. Results and discussion

Nyquist plots for the grease samples at 60 °C during the 3-Heating temperature sweep are shown as examples in Fig. 3. The equivalent electrical circuits selected for fitting the various impedance spectra are listed in ESI Figure S1. The physical significance of all the circuits used in this study is also explained in ESI Table S1.

Almost all of the grease samples exhibited the semi-circular spectral feature (originating from the complex impedance of the bulk), leading to a selection of RP circuit components to represent the bulk electrical properties. Only for the grease with EMIM-TFSI, an offset from zero was observed on the real axis, motivating the use of only a resistor element to represent the bulk electrical properties. This shows that for the grease with EMIM-TFSI the bulk capacitance is negligible.

The nature of the equivalent circuit representing the bulk remains stable over time and temperature for all the samples, though, of course, the fitted values of the circuit components change. Bulk conductivity is extracted from the appropriate value of the bulk resistance component (examples of which are labeled as R_B in Fig. 3). The other circuit components (detailed in ESI Figure S1) are characteristic of interfacial processes. Changes were observed, over time and temperature, in the nature of the circuit representing the sample-electrode interface, reflecting the complexity and dynamics of this region. All the grease samples, other than the base grease itself, show an interfacial spectrum that a double-layer capacitance and a charge transfer resistor in parallel can well represent. The interfacial spectral features for greases with solid additives become evident only some time into the 1-Heating temperature sweep. The greases with ILs, other than P-BEHP, exhibit an additional spectral feature that can be represented by a diffusion component (either a Warburg element or a CPE) in the equivalent circuit. For the greases with copper and P-BOB at lower temperatures, the charge transfer resistor associated with the double-layer capacitance appears to become too high to be captured within the measured frequency range, leading to the spectra being better fitted using only a CPE element. It must be noted that the spectral features corresponding to the interfacial structuring (low frequency) observed within the tested frequency range are applied solely to provide a good fit to this data and allow the higher frequency features (bulk conductivity) to be accurately captured. Therefore, the choice of equivalent circuits for the interfacial region is only indicative and not intended to give detailed information on the structuring and self-assembly at the electrode interface. These

interfacial characteristics, while important for the grease function, are not the focus of this work. More in-depth studies would be needed to reveal the interfacial structuring and its electrical characteristics.

The conductivity values obtained during the four temperature sweeps for all the IL grease samples are shown in ESI Figure S4, and for the greases with solid additives are shown in Fig. 4. It can be observed that there is a certain dependence on the sweep number, particularly in the case of the solid additives, which is likely related to a conditioning process. The base grease (without any additives) exhibits only a very low conductivity despite the ionic nature of its thickener (ESI Figure S4a). However, it exhibits an increasing conductivity with temperature. This can be attributed to the thermally induced increase in mobility of the charge carriers (possibly dissociated lithium ions from the thickener) together with a decrease in rheological resistance (decreased viscosity with increasing temperature) of the grease complex. This shows that although lithium is part of the thickener system that gives the grease its structural properties, its dissociated ionic form is one of the advantages when developing electrically conductive greases.

Fig. 5 compares the temperature-dependent conductivity of the LiX greases with solid additives, during the 3-Heating and 4-Cooling temperature sweeps. It can be seen that the addition of solid additives to the grease increases the conductivity by several orders of magnitude. The grease containing carbon black additive shows an inverse conductivity dependence on temperature. Similar behavior has been reported for pure graphite [72], as well as for semiconductor graphite/epoxy composites [73]. This indicates that the conductivity mechanism is dominated by the conduction through a graphite-like carbon network in the grease matrix, as reported for CNT-based greases [30]. This network appears to form during the 1-Heating temperature sweep, during which the conductivity is much lower than the following temperature sweeps (Fig. 4(b)). The network formation is presumably facilitated by reduced viscosity at the higher temperature end of the first heating sweep, allowing interactions to be built between the dispersed carbon black aggregates.

In the case of grease with copper powder, the conductivity is lower than for the carbon black case (Fig. 5). The conductivity of copper grease increases with temperature, which is inconsistent with the intrinsic electrical conductivity of copper metal [74]. This shows that the grease sample with copper does not follow a metallic electrical conductivity pathway but instead follows an ionic conductivity pathway. Adsorption of the anionic component of the grease thickener to the metal (Cu) surface may lead to the liberation of more dissociated lithium ions, resulting in an increased conductivity compared to the base grease. Released copper ions may also contribute. As in the case of the carbon black additive, the conductivity during the 1-Heating sweep is quite low (Fig. 4(a)), suggesting that the suggested anion-metal association is thermally assisted. It is also possible that the particles are able to align more easily, or partially aggregate, with the applied field, leading to the hybrid conduction mechanism alluded to above — that is to say, polarization in the metallic particles with correspondingly facilitated ion separation.

Fig. 6 shows the comparison of temperature-dependent conductivity for LiX greases with IL additives, during the 3-Heating and 4-Cooling temperature sweeps. The addition of ILs to the grease also results in an increase in conductivity by several orders of magnitude. The direct relation between temperature and conductivity confirms that the ionic conductivity pathway is followed. The increase in conductivity compared to the neat grease can be seen to be highly dependent on the choice of IL. The EMIM-TFSI additive results in the highest conductivity, up to three orders of magnitude higher than the next most conductive grease sample (LiX + P-DCA), which is over an order of magnitude more conductive than the least conductive grease sample (LiX + P-BMB). The conductivity of EMIM-TFSI grease is also greater than that of the grease with carbon black additive, which is otherwise the most conductive sample. Its high conductivity presumably reflects a greater degree of dissociation of the ions (lower ion-pairing). By
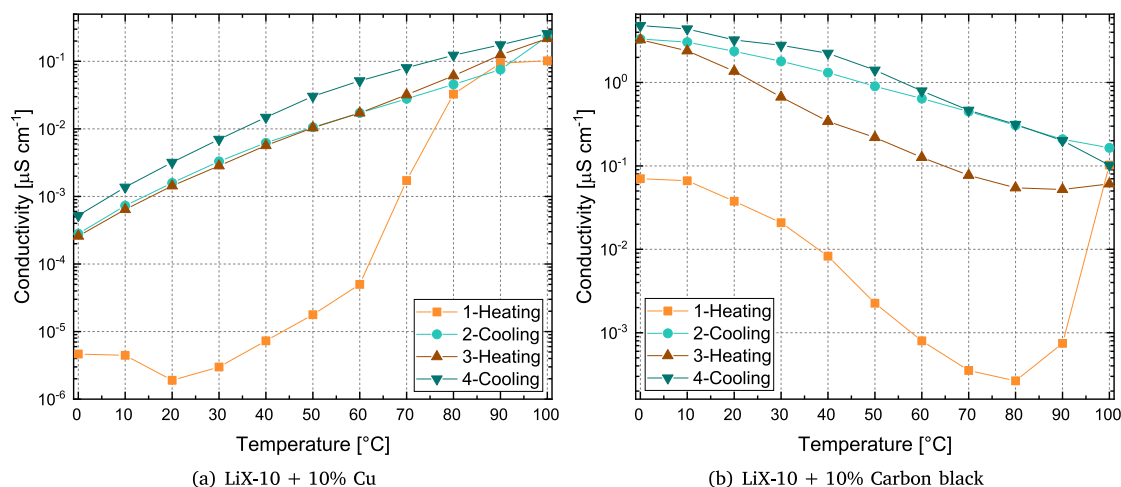
Fig. 4. Bulk electrical Conductivity as a function of temperature for grease samples with solid additives during the four temperature cycles.
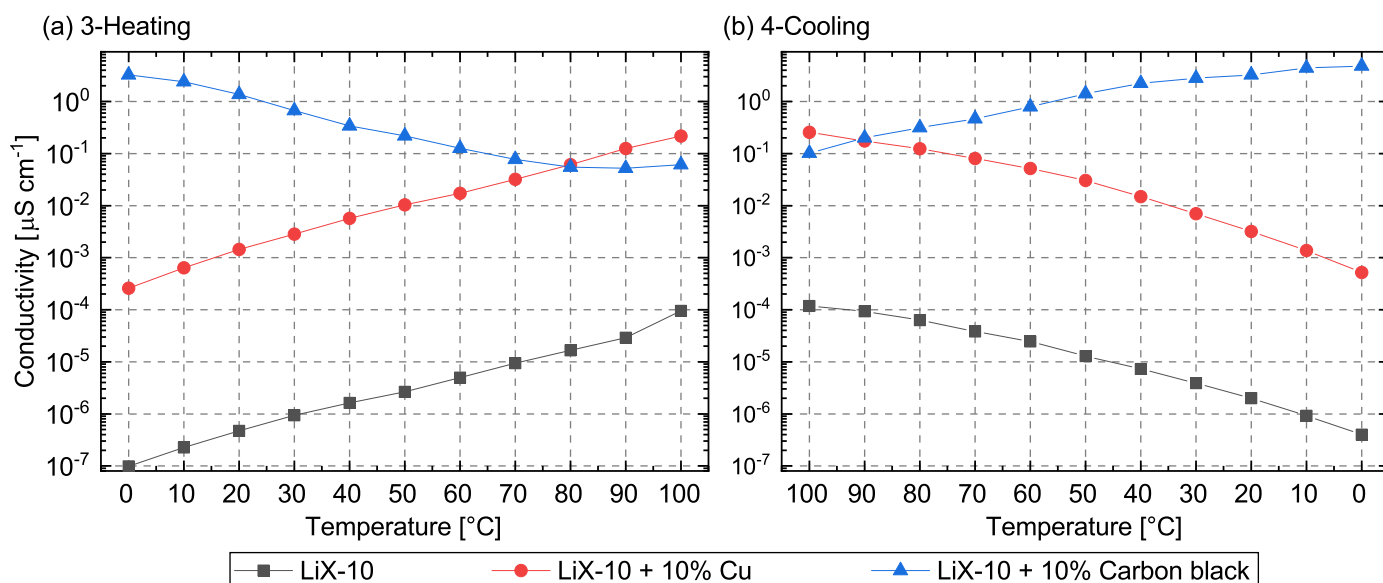

Fig. 5. Bulk electrical conductivity of the grease samples with solid additives, i.e., copper and carbon black, as a function of temperature during 3-Heating (a), and 4-Cooling (b) temperature sweeps.

the same token, the larger proportional increase in conductivity of the other ILs with temperature suggests that increased temperature leads not only to reduced rheological resistance but also to an increase in ion dissociation.

The conductivity of neat ILs during the 3-Heating temperature sweep is shown in Fig. 7. The selection of equivalent electrical circuits for the neat IL impedance spectra is shown in ESI Figure S3. The ionic conductivity showed negligible variance between the four temperature sweeps, reflecting the much simpler liquid structure. EMIM-TFSI exhibits the highest conductivity of all ILs, with the results congruent with values reported by Widegren et al. [68], measured using a commercial conductivity cell based on the AC impedance bridge technique. The high conductivity of EMIM-TFSI can be attributed to the less bulky ions compared to the phosphonium ILs, therefore allowing for better ionic mobility combined with a higher degree of ion dissociation. The conductivity values for P-BOB and P-BMB are also in good agreement with previously reported data [65,66].

Here it can be seen that the sequence of conductivity (most conductive to least conductive) of neat ILs is not the same as the sequence of conductivity when the same ILs are added to the grease. As a neat IL, P-BEHP has much lower conductivity than P-BOB (Fig. 7), whereas the conductivity of grease with P-BEHP is higher than that of the grease with P-BOB (Fig. 6). The reason for this can be attributed to P-BEHP being the only IL (of those tested) that is miscible with the base oil, allowing conductivity through the oil phase rather than solely through polar regions associated with the LiX thickener. Supporting this hypothesis is the observation that the P-BEHP grease does not exhibit any hysteresis (ESI Figure S4e) during the temperature cycling, thus showing no initial conditioning stage as evident for all other grease samples. The conduction mechanisms thus do not only depend on the liquid properties of the ILs, but rather upon how and where they are distributed in the grease matrix. This is in correlation with molecular dynamics simulations presented by Martinez-Crespo et al. which have identified the solvation of the salt as a major determinant of charge transport in a mixture [75]. Therefore, the conductivity trend for greases with IL additives cannot be directly equated to the conductivity of neat ILs. In addition to the degree of ion dissociation, the self-assembly/solvation properties of the ions with the grease matrix or the base oil must also be considered while evaluating the conductivity mechanism of greases doped with ILs.
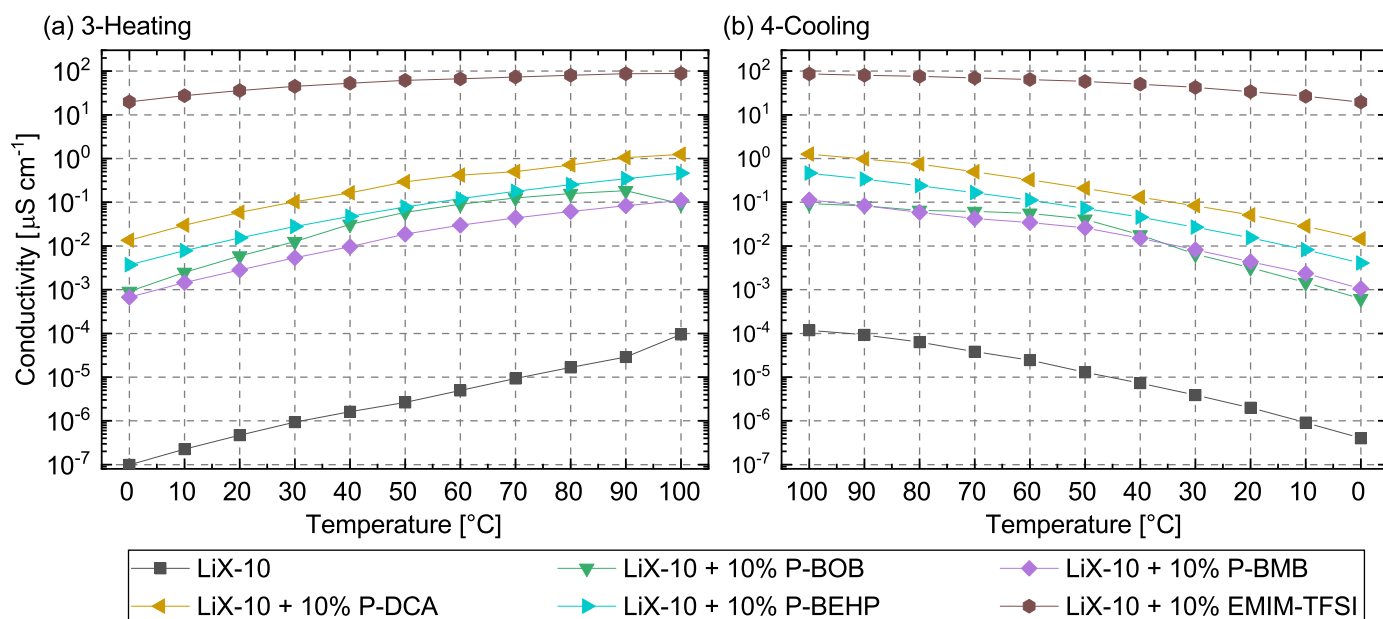
Fig. 6. Bulk electrical conductivity of the grease samples with ILs as a function of temperature during 3-Heating (a), and 4-Cooling (b) temperature sweeps.
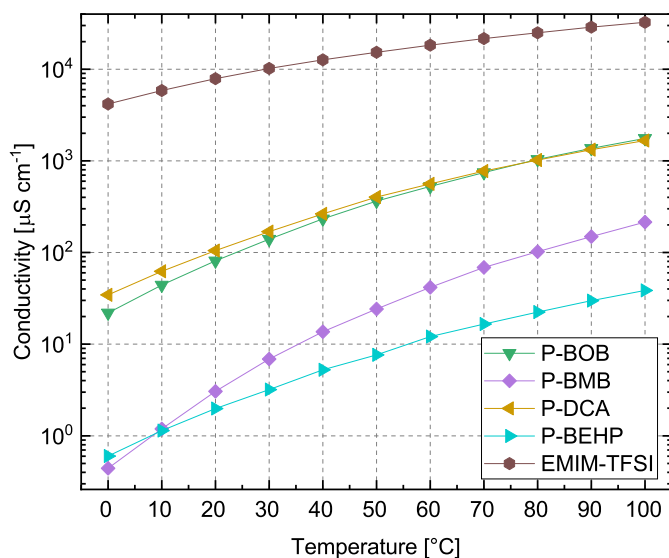

Fig. 7. The conductivity values obtained for different neat ILs during the 3-Heating temperature sweep.

From an application perspective, the conductivity requirement for lubricants could be pretty diverse, as evident from the various suggested functional conductivity ranges [19,21,22]. While all greases measured in this work, other than the grease with EMIM-TFSI, satisfy the suggested limit (> 1 μS cm⁻¹) for preventing tribo-corrosion related surface damages [19], they exceed the functional range suggested by Gao et al. for high conductivity lubricating oils (3×10^{-5} to 2×10^{-4} μS cm⁻¹) [21]. Gaining an understanding of the conductivity pathway (through the grease matrix or oil phase) is essential for predicting the actual conductivity performance of the grease when in contact. This is because the oil bleed/release mechanisms determine the actual lubricant composition in the nanometer scale contact gap [76,77]. Employing ILs as the conductivity medium in greases presents the possibility of tuning the grease conductivity over several orders of

magnitude to satisfy the exact application requirements by choosing the appropriate IL and concentration. This also paves a path for employing conductivity additives without compromising on tribological performance of the grease. For example, P-BOB, in addition to enhancing the electrical conductivity of the grease, has also been shown to reduce friction and wear [43].

The impedance measurements described and their subsequent analysis demonstrates that EIS's functionality can be extended to conductive greases based on both ionic and non-ionic additives. Compared to the commonly used resistive or capacitive sensing techniques, a thorough evaluation of both the real and imaginary part of the impedance, EIS allows for much more detail to be extracted about the electrical properties of the bulk grease sample and the interfacial structuring on the electrode surface. This method is beneficial for complex systems where the bulk impedance is frequency-dependent. It allows for the accurate measurement of temperature and time-dependent conductivity by isolating the contributions of the interfacial features. However, the 80 μm electrode gap is not comparable to the nanometer scale lubricant film thickness in a tribological contact. Contact-level testing would be required to assess the electrical behavior of greases in realistic tribological contacts, which would also take grease lubrication characteristics, such as shearing and oil bleed, into account.

4. Conclusions

Characterizing the electrical properties of lubricating greases is essential in developing electrically conductive greases for e-mobility applications. This paper shows how ionic liquids (ILs) can enhance electrical conductivity of greases. LiX greases are complex colloidal systems, but the conductivity mechanisms can nonetheless be understood in terms of the additive architecture. In the case of the carbon black additive, temperature cycling enabled an inverse conductivity-temperature relationship due to the conductive carbon network formation across the grease, facilitated by reduced viscous forces at high temperatures.

The addition of IL to grease at a concentration of 10 wt% resulted in an increase in conductivity by three to six orders of magnitude, reflecting significant differences in both the conductivity of the pure ILs themselves as well as in their ability to interact with the grease

materials — for example, as an ionic solute in the oil or in association with the polar regions of the matrix. Thus, in addition to ion dissociation, the self-assembly properties of ions with the grease matrix are critical in defining the ion mobility and thereby the conductivity of the grease. The findings allow for the systematic control and study of the electrical properties of greases and provide insight into the conductivity pathways through the complex material — which can be either via the matrix itself, or via the IL-containing oil phase.

The electrochemical impedance spectroscopy (EIS) methodology presented in this study allows for the measurement of grease bulk conductivity over a wide range of magnitudes, regardless of the nature of additives (ionic or non-ionic). It also allows for facile investigation and control of both temperature and temporal response. In contrast to conventional conductivity measurement, multi-frequency impedance spectra (both real and imaginary) and analysis of the ensuing equivalent electrical circuits serves as an effective means to extract the bulk electrical properties by isolating them from the electrical contributions of the electrode-sample interfacial features. The approach also provides an understanding of how the conductivity mechanisms vary with temperature and how the heat treatment of the grease can be used to tune the electrical properties. Future work will also address the interfacial responses of these systems, which are of great interest for understanding the boundary layer response.

CRediT authorship contribution statement

Akepati Bhaskar Reddy: Conceptualization, Formal analysis, Methodology, Visualization, Writing – original draft. **Faiz Ullah Shah:** Investigation, Writing – review & editing. **Johan Leckner:** Resources, Writing – review & editing. **Mark W. Rutland:** Supervision, Writing – review & editing. **Sergei Glavatskih:** Conceptualization, Project administration, Supervision, Writing – review & editing.

Declaration of competing interest

The authors declare the following financial interests/personal relationships which may be considered as potential competing interests: Sergei Glavatskih and Faiz Ullah Shah have patents #JP5920900 and #SE535675 issued to KTH.

Data availability

Data will be made available on request.

Acknowledgments

Appendix A. Supplementary data

Supplementary material related to this article can be found online at https://doi.org/10.1016/j.colsurfa.2023.132875.

References

[1] T. Welton, Ionic liquids: a brief history, Biophys. Rev. 10 (3) (2018) 691–706, http://dx.doi.org/10.1007/s12551-018-0419-2.

[2] N.V. Plechkova, K.R. Seddon, Applications of ionic liquids in the chemical industry, Chem. Soc. Rev. 37 (1) (2008) 123–150, http://dx.doi.org/10.1039/B006677J.

[3] K.R. Seddon, Ionic liquids for clean technology, J. Chem. Technol. Biotechnol. 68 (4) (1997) 351–356, http://dx.doi.org/10.1002/(SICI)1097-4660(199704)68:4<351::AID-JCTB613>3.0.CO;2-4.

[4] M.T. Donato, R. Colaço, L.C. Branco, B. Saramago, A review on alternative lubricants: Ionic liquids as additives and deep eutectic solvents, J. Mol. Liq. 333 (2021) 116004, http://dx.doi.org/10.1016/j.molliq.2021.116004.

[5] H. Xiao, Ionic liquid lubricants: Basics and applications, Tribol. Trans. 60 (1) (2017) 20–30, http://dx.doi.org/10.1080/10402004.2016.1142629.

[6] C. Zhang, F. Li, Z. Yang, X. Wang, G. Chen, Z. Lu, L. Jia, Q. Yu, M. Cai, Comparing tribology properties of halogen-free ionic liquid, halogen-containing ionic liquid, and PAO 10 lubricants for steel–Al2024 friction contact at room temperature and high temperature, J. Mol. Liq. 323 (2021) 115041, http://dx.doi.org/10.1016/j.molliq.2020.115041.

[7] J.L. Teh, R. Walvekar, T. Nagarajan, Z. Said, M. Khalid, N.M. Mubarak, A review on the properties and tribological performance of recent non-aqueous miscible lubricants, J. Mol. Liq. 366 (2022) 120274, http://dx.doi.org/10.1016/j.molliq.2022.120274.

[8] A.G. Tuero, C. Sanjurjo, N. Rivera, J.L. Viesca, R. González, A.H. Battez, Electrical conductivity and tribological behavior of an automatic transmission fluid additised with a phosphonium-based ionic liquid, J. Mol. Liq. 367 (2022) 120581, http://dx.doi.org/10.1016/j.molliq.2022.120581.

[9] A. Jagenbrein, Investigations of Bearing Failures Due to Electric Current Passage (Doctoral dissertation), Technische Universit.

[10] H. Prashad, 4 - Diagnosis and cause analysis of rolling-element bearings failure in electric power equipment, in: H. Prashad (Ed.), Solving Tribology Problems in Rotating Machines, Woodhead Publishing, 2006, pp. 56–66, http://dx.doi.org/10.1533/9781845691110.56.

[11] F. He, G. Xie, J. Luo, Electrical bearing failures in electric vehicles, Friction 8 (1) (2020) 4–28, http://dx.doi.org/10.1007/s40544-019-0356-5.

[12] D. Busse, J. Erdman, R. Kerkman, D. Schlegel, G. Skibinski, Characteristics of shaft voltage and bearing currents, IEEE Ind. Appl. Mag. 3 (6) (1997) 21–32, http://dx.doi.org/10.1109/2943.628116.

[13] H. Tischmacher, S. Gattermann, M. Kriese, E. Wittek, Bearing wear caused by converter-induced bearing currents, in: IECON 2010 - 36th Annual Conference on IEEE Industrial Electronics Society, pp. 784–791, http://dx.doi.org/10.1109/IECON.2010.5675212.

[14] S. Gunderson, G. Fultz, C.E. Snyder, J. Wright, L. Gschwender, S. Heidger, The effect of water content on the dielectric strength of polyalphaolefin (PAO) coolants, IEEE Trans. Dielectr. Electr. Insul. 18 (1) (2011) 295–302, http://dx.doi.org/10.1109/TDEI.2011.5704521.

[15] X. Wang, Z.D. Wang, Particle effect on breakdown voltage of mineral and ester based transformer oils, in: 2008 Annual Report Conference on Electrical Insulation and Dielectric Phenomena, pp. 598–602, http://dx.doi.org/10.1109/CEIDP.2008.4772859.

[16] H. Prashad, T.S.R. Murthy, The deterioration of lithium greases under the influence of electric current—an investigation, Lubr. Sci. 10 (4) (1998) 323–342, http://dx.doi.org/10.1002/ls.3010100405.

[17] A. Gonda, R. Capan, D. Bechev, B. Sauer, The influence of lubricant conductivity on bearing currents in the case of rolling bearing greases, Lubricants 7 (12) (2019) 108, http://dx.doi.org/10.3390/lubricants7120108.

[18] J. Suzumura, Prevention of electrical pitting on rolling bearings by electrically conductive grease, Q. Rep. RTRI 57 (1) (2016) 42–47, http://dx.doi.org/10.2219/rtriqr.57.1_42.

[19] H. Prashad, Determination of time span for the appearance of flutes on the track surface of rolling-element bearings under the influence of electric current, Tribol. Trans. 41 (1) (1998) 103–109, http://dx.doi.org/10.1080/10402009808983727.

[20] Y. Chen, S. Jha, A. Raut, W. Zhang, H. Liang, Performance characteristics of lubricants in electric and hybrid vehicles: A review of current and future needs, Front. Mech. Eng. 6 (2020) http://dx.doi.org/10.3389/fmech.2020.571464.

[21] Z. Gao, L. Salvi, S. Flores-Torres, High Conductivity Lubricating Oils for Electric and Hybrid Vehicles, US Patent App. 15/725,635US Patent App. 15/725,635, 2018.

[22] Z. Gao, L. Salvi, S. Flores-Torres, Low Conductivity Lubricating Oils for Electric and Hybrid Vehicles, US Patent App. 15/725,670, 2018.

[23] R. Shah, S. Tung, R. Chen, R. Miller, Grease performance requirements and future perspectives for electric and hybrid vehicle applications, Lubricants 9 (4) (2021) 40, http://dx.doi.org/10.3390/lubricants9040040.

[24] C. Roman, C. Valencia, J.M. Franco, AFM and SEM assessment of lubricating grease microstructures: Influence of sample preparation protocol, frictional working conditions and composition, Tribol. Lett. 63 (2) (2016) http://dx.doi.org/10.1007/s11249-016-0710-y.

[25] 2022 NLGI Grease Production Survey Report, Report, Grease Technology Solutions, LLC, USA.

[26] Z. Cao, Y. Xia, X. Ge, Conductive capacity and tribological properties of several carbon materials in conductive greases, Ind. Lubr. Tribol. 68 (5) (2016) 577–585, http://dx.doi.org/10.1108/ILT-07-2015-0113.

[27] P.L. Zhang, G.G. Wang, Y.J. Zhao, H. Wu, Y.Q. Xia, Study of conductive and friction properties of grease containing carbon black additive, Adv. Mater. Res. 1120–1121 (2015) 586–589, http://dx.doi.org/10.4028/www.scientific.net/AMR.1120-1121.586.

[28] W. Millar, Z.M. Aman, R. Atkin, H. Li, Graphite infused ionic liquid greases, Colloids Surf. A 653 (2022) 130017, http://dx.doi.org/10.1016/j.colsurfa.2022.130017.

[29] G. Christensen, J. Yang, D. Lou, G. Hong, H. Hong, C. Tolle, C. Widener, C. Bailey, R. Hrabe, H. Younes, Carbon nanotubes grease with high electrical conductivity, Synth. Met. 268 (2020) 116496, http://dx.doi.org/10.1016/j.synthmet.2020.116496.

[30] H. Hong, D. Thomas, A. Waynick, W. Yu, P. Smith, W. Roy, Carbon nanotube grease with enhanced thermal and electrical conductivities, J. Nanoparticle Res. 12 (2) (2010) 529–535, http://dx.doi.org/10.1007/s11051-009-9803-y.

[31] L. Vanyorek, D. Kiss, A. Prekob, B. Fiser, A. Potyka, G. Nemeth, L. Kuzsela, D. Drees, A. Trohak, B. Viskolcz, Application of nitrogen doped bamboo-like carbon nanotube for development of electrically conductive lubricants, J. Mater. Res. Technol. 8 (3) (2019) 3244–3250, http://dx.doi.org/10.1016/j.jmrt.2019.05.012.

[32] X. Ge, Y. Xia, X. Feng, Influence of carbon nanotubes on conductive capacity and tribological characteristics of poly(ethylene glycol-ran-propylene glycol) monobutyl ether as base oil of grease, J. Tribol. 138 (1) (2015) http://dx.doi.org/10.1115/1.4031232.

[33] H. Younes, D. Lou, H. Hong, H. Chen, H. Liu, Y. Qiang, Manufacturable novel nanogrease with superb physical properties, Nanomanufacturing Metrol. 4 (4) (2021) 289–297, http://dx.doi.org/10.1007/s41871-021-00111-9.

[34] X. Ge, Y. Xia, Z. Shu, X. Zhao, Conductive grease synthesized using nanometer ATO as an additive, Friction 3 (1) (2015) 56–64, http://dx.doi.org/10.1007/s40544-015-0073-7.

[35] W. Oh, Preventing VFD/AC Drive-Induced Electrical Damage to AC Motor Bearings, Technical Paper, Electro Static Technology, 2018, https://est-aegis.com/TechPaper.pdf.

[36] X. Fan, Y. Xia, L. Wang, J. Pu, T. Chen, H. Zhang, Study of the conductivity and tribological performance of ionic liquid and lithium greases, Tribol. Lett. 53 (1) (2014) 281–291, http://dx.doi.org/10.1007/s11249-013-0266-z.

[37] X. Fan, L. Wang, Highly conductive ionic liquids toward high-performance space-lubricating greases, ACS Appl. Mater. Interfaces 6 (16) (2014) 14660–14671, http://dx.doi.org/10.1021/am503941e.

[38] X. Ge, Y. Xia, X. Feng, Y. Song, X. Fan, Electrical conductivities and tribological properties of lithium salts conductive grease, Jixie Gongcheng Xuebao (Journal of Mechanical Engineering) 51 (15) (2015) 61–66, http://dx.doi.org/10.3901/JME.2015.15.061.

[39] X. Fan, L. Wang, Y. Xia, Oil-soluble lithium salts as novel lubricant additives towards improving conductivity and tribological performance of bentone grease, Lubr. Sci. 27 (6) (2015) 359–368, http://dx.doi.org/10.1002/ls.1286.

[40] L.N. Wu, Y.Q. Xia, X. Feng, H. Wu, Electrical conductivity of ionic liquids as lubricating grease, Mocaxue Xuebao (Tribology) 34 (2) (2014) 198–202.

[41] X. Fan, Y. Xia, L. Wang, Tribological properties of conductive lubricating greases, Friction 2 (4) (2014) 343–353, http://dx.doi.org/10.1007/s40544-014-0062-2.

[42] M.F. Fox, M. Priest, Tribological properties of ionic liquids as lubricants and additives. Part 1: Synergistic tribofilm formation between ionic liquids and tricresyl phosphate, Proc. Inst. Mech. Eng. J 222 (3) (2008) 291–303, http://dx.doi.org/10.1243/13506501jet387.

[43] M. Ploss, Y. Tian, S. Yoshikawa, R. Westbroek, J. Leckner, S. Glavatskih, Tribological performance of non-halogenated phosphonium ionic liquids as additives to polypropylene and lithium-complex greases, Tribol. Lett. 68 (1) (2020) http://dx.doi.org/10.1007/s11249-019-1240-1.

[44] Z. Wang, Y. Xia, Z. Liu, Comparative study of the tribological properties of ionic liquids as additives of the attapulgite and bentone greases, Lubr. Sci. 24 (4) (2012) 174–187, http://dx.doi.org/10.1002/ls.1173.

[45] M. Cai, Z. Zhao, Y. Liang, F. Zhou, W. Liu, Alkyl imidazolium ionic liquids as friction reduction and anti-wear additive in polyurea grease for steel/steel contacts, Tribol. Lett. 40 (2) (2010) 215–224, http://dx.doi.org/10.1007/s11249-010-9624-2.

[46] A. García Tuero, M. Bartolomé, D. Gonçalves, J.L. Viesca, A. Fernández-González, J.H.O. Seabra, A. Hernández Battez, Phosphonium-based ionic liquids as additives in calcium/lithium greases, J. Mol. Liq. 338 (2021) 116697, http://dx.doi.org/10.1016/j.molliq.2021.116697.

[47] ASTM International, Standard Test Method for Electrical Conductivity of Liquid Hydrocarbons by Precision Meter, ASTM D4308-21, ASTM International, 2021, http://dx.doi.org/10.1520/D4308-21.

[48] ISO, Paints and Varnishes — Determination of Electrical Conductivity and Resistance, ISO 15091:2019, International Organization for Standardization (ISO), 2019.

[49] ASTM International, Standard Test Methods for Electrical Conductivity of Aviation and Distillate Fuels, ASTM D2624-22, ASTM International, 2022, http://dx.doi.org/10.1520/D2624-22.

[50] A.A. Gundyrev, A.Y. Kizas, Electrical conductivity of soap-base greases and dispersions, Chem. Technol. Fuels Oils 16 (6) (1980) 403–406, http://dx.doi.org/10.1007/BF00727163.

[51] J.R. Macdonald, Impedance spectroscopy, Ann. Biomed. Eng. 20 (3) (1992) 289–305.

[52] M. Grossi, B. Riccò, Electrical impedance spectroscopy (EIS) for biological analysis and food characterization: a review, J. Sens. Sens. Syst. 6 (2) (2017) 303–325, http://dx.doi.org/10.5194/jsss-6-303-2017.

[53] J. Wang, Study of electrode reactions and interfacial properties, in: Analytical Electrochemistry, third ed., John Wiley & Sons, Ltd, 2006, pp. 29–66, http://dx.doi.org/10.1002/0471790303.ch2.

[54] B.J. Christensen, T. Coverdale, R.A. Olson, S.J. Ford, E.J. Garboczi, H.M. Jennings, T.O. Mason, Impedance spectroscopy of hydrating cement-based materials: Measurement, interpretation, and application, J. Am. Ceram. Soc. 77 (11) (1994) 2789–2804, http://dx.doi.org/10.1111/j.1151-2916.1994.tb04507.x.

[55] P. Gu, P. Xie, J.J. Beaudoin, R. Brousseau, A.C. impedance spectroscopy (i): A new equivalent circuit model for hydrated portland cement paste, Cem. Concr. Res. 22 (5) (1992) 833–840, http://dx.doi.org/10.1016/0008-8846(92)90107-7.

[56] P.J. Tumidajski, Electrical conductivity of portland cement mortars, Cem. Concr. Res. 26 (4) (1996) 529–534, http://dx.doi.org/10.1016/0008-8846(96)00027-0.

[57] W.J. McCarter, S. Garvin, N. Bouzid, Impedance measurements on cement paste, J. Mater. Sci. Lett. 7 (10) (1988) 1056–1057, http://dx.doi.org/10.1007/BF00720825.

[58] W.J. McCarter, R. Brousseau, The A.C. response of hardened cement paste, Cem. Concr. Res. 20 (6) (1990) 891–900, http://dx.doi.org/10.1016/0008-8846(90)90051-X.

[59] C.A. Scuderi, T.O. Mason, H.M. Jennings, Impedance spectra of hydrating cement pastes, J. Mater. Sci. 26 (2) (1991) 349–353, http://dx.doi.org/10.1007/BF00576526.

[60] A.D. Hixson, L.Y. Woo, M.A. Campo, T.O. Mason, E.J. Garboczi, Intrinsic conductivity of short conductive fibers in composites by impedance spectroscopy, J. Electroceram. 7 (3) (2001) 189–195, http://dx.doi.org/10.1023/A:1014487129118.

[61] X. Qian, N. Gu, Z. Cheng, X. Yang, E. Wang, S. Dong, Methods to study the ionic conductivity of polymeric electrolytes using a.c. impedance spectroscopy, J. Solid State Electrochem. 6 (1) (2001) 8–15, http://dx.doi.org/10.1007/s100080000190.

[62] S.S. Wang, S.P. Maheswari, S.C. Tung, AC impedance measurements of the resistance and capacitance of lubricants, A S L E Trans. 30 (4) (1986) 436–443, http://dx.doi.org/10.1080/05698198708981777.

[63] J. Shu, K. Harris, B. Munavirov, R. Westbroek, J. Leckner, S. Glavatskih, Tribology of polypropylene and li-complex greases with ZDDP and MoDTC additives, Tribol. Int. 118 (2018) 189–195, http://dx.doi.org/10.1016/j.triboint.2017.09.028.

[64] J. Leckner, R. Westbroek, Polypropylene—a new thickener technology for energy efficient lubrication, NLGI Spokesm. 81 (1) (2017) 34–56.

[65] M.R. Shimpi, P. Rohlmann, F.U. Shah, S. Glavatskih, O.N. Antzutkin, Transition anionic complex in trihexyl(tetradecyl)phosphonium-bis(oxalato)borate ionic liquid – revisited, Phys. Chem. Chem. Phys. 23 (2021) 6190–6203, http://dx.doi.org/10.1039/D0CP05845A.

[66] F.U. Shah, S. Glavatskih, D.R. MacFarlane, A. Somers, M. Forsyth, O.N. Antzutkin, Novel halogen-free chelated orthoborate-phosphonium ionic liquids: synthesis and tribophysical properties, Phys. Chem. Chem. Phys. 13 (2011) 12865–12873, http://dx.doi.org/10.1039/c1cp21139k.

[67] Y. Zhou, J. Qu, Ionic liquids as lubricant additives: A review, ACS Appl. Mater. Interfaces 9 (4) (2017) 3209–3222, http://dx.doi.org/10.1021/acsami.6b12489.

[68] J.A. Widegren, E.M. Saurer, K.N. Marsh, J.W. Magee, Electrolytic conductivity of four imidazolium-based room-temperature ionic liquids and the effect of a water impurity, J. Chem. Thermodyn. 37 (6) (2005) 569–575, http://dx.doi.org/10.1016/j.jct.2005.04.009.

[69] M.E. Orazem, B. Tribollet, Electrical circuits, in: Electrochemical Impedance Spectroscopy, John Wiley & Sons, Ltd, 2008, pp. 61–72, http://dx.doi.org/10.1002/9780470381588.ch4.

[70] M.E. Orazem, B. Tribollet, Time-constant dispersion, in: Electrochemical Impedance Spectroscopy, John Wiley & Sons, Ltd, 2008, pp. 233–263, http://dx.doi.org/10.1002/9780470381588.ch13.

[71] M.E. Orazem, B. Tribollet, Diffusion impedance, in: Electrochemical Impedance Spectroscopy, John Wiley & Sons, Ltd, 2008, pp. 183–210, http://dx.doi.org/10.1002/9780470381588.ch11.

[72] A. Radoń, P. Włodarczyk, D. Łukowiec, Structure, temperature and frequency dependent electrical conductivity of oxidized and reduced electrochemically exfoliated graphite, Physica E 99 (2018) 82–90, http://dx.doi.org/10.1016/j.physe.2018.01.025.

[73] J.M.L. Reis, S.A. Martins, H.S. da Costa Mattos, Combination of temperature and electrical conductivity on semiconductor graphite/epoxy composites, J. Braz. Soc. Mech. Sci. Eng. 42 (8) (2020) 404, http://dx.doi.org/10.1007/s40430-020-02487-z.

[74] L. Lu, Y. Shen, X. Chen, L. Qian, K. Lu, Ultrahigh strength and high electrical conductivity in copper, Science 304 (5669) (2004) 422–426, http://dx.doi.org/10.1126/science.1092905.

[75] P. Martínez-Crespo, M. Otero-Lema, O. Cabeza, H. Montes-Campos, L.M. Varela, Structure, dynamics and ionic conductivities of ternary ionic liquid/lithium salt/DMSO mixtures, J. Mol. Liq. 359 (2022) 119188, http://dx.doi.org/10.1016/j.molliq.2022.119188.

[76] P. Baart, B. van der Vorst, P.M. Lugt, R.A.J. van Ostayen, Oil-bleeding model for lubricating grease based on viscous flow through a porous microstructure, Tribol. Trans. 53 (3) (2010) 340–348, http://dx.doi.org/10.1080/10402000903283326.

[77] A. Saatchi, P.J. Shiller, S.A. Eghtesadi, T. Liu, G.L. Doll, A fundamental study of oil release mechanism in soap and non-soap thickened greases, Tribol. Int. 110 (2017) 333–340, http://dx.doi.org/10.1016/j.triboint.2017.02.004.